Enhancing the Provision of Ancillary Services from Storage Systems using Smart Transformer and Smart Meters

Fabrizio Sossan, Konstantina Christakou, Mario Paolone
Distributed Electrical Systems Laboratory
École Polytechnique Fédérale de Lausanne (EPFL)
Lausanne, Switzerland

Xiang Gao, Marco Liserre
Chair of Power Electronics
Christian Albrechts Universität zu Kiel
Kiel, Germany

***Abstract*—The Smart Transformer, a solid-state transformer with control and communication functionalities, can be the ideal solution for integrating storage into the grid. By leveraging the knowledge of the grid state of distribution grids thanks to smart meters and/or dedicated remote terminal units, in the paper, it is proposed a control strategy for a MV/LV smart transformer (ST) with integrated storage to achieve: i) dispatched-by-design operation of the LV network by controlling the ST active power set-point on the MV power converter, and ii) voltage regulation of both MV and LV networks by controlling the reactive power injections of both LV and MV converter. The former is achieved by dispatching the active power flow of the LV network according to a profile established the day before the operation, called *dispatch plan*, with the objective of reducing the amount of regulating power required to operate the grid. It is based on the use of forecast to compute a dispatch plan, and a tracking problem to compensate in real-time the mismatch between realization and dispatch plan by taking advantage of the storage capacity. The latter is achieved by using sensitivity coefficients, which are calculated from the state of the grid and integrating the information on the network topology. The problem formulation is given in the paper, and the proof-of-concept is shown by simulation using the IEEE 34 nodes test feeder and the CIGRE Low Voltage reference network.**

I. Introduction

As defined in the existing literature, the concept of Active Distribution Networks (ADNs) refers to electrical grids where the energy resources (i.e., distributed generation, storage, loads, etc.) are actively controlled by a suitable Energy Management System (EMS), in order to achieve specific operation objectives (e.g., [1], [2]). These objectives typically refer to optimal voltage control, management of line-congestion, local load balance, aggregation and dispatching of local feeders, losses minimization, etc. All these functionalities are significantly improved if the knowledge of the network state is available. As these functionalities are deployed in time horizons that vary between few hundreds of ms (fault management) to few tens of seconds (voltage control and line congestions), they might require the knowledge of the network state with relatively high refresh rates. In this respect, the massive adoption in ADNs of end-user smart metering and/or dedicated remote terminal units (such as Phasor Measurement Units) enables EMS to have access to the grid state with high time resolution, accuracy and low latency [3]. As a consequence, these monitoring technologies enables the definition of optimal control strategies that also take advantage of new flexible elements composed by grid-connected battery energy storage systems (BESS). The conventional way of deploying grid-connected battery energy storage systems (BESSs) in distribution networks consists in connecting the battery DC bus to the AC side through a DC/AC power converter. In this paper, we explore an alternative setup, where the storage capacity is connected to the DC bus of a smart transformer (ST) interfacing a low voltage (LV) to a medium voltage (MV) system. This configuration, although more complex than a distribution system equipped with a ST or grid-connected BESS only, achieves a full decoupling of the flows of the two electrical grids, a feature that allows to extend the class of ancillary services that distribution systems can provide to the upper grid layer, as shown in this paper.

A BESS consists in a battery cells stack connected to the AC side with a DC/AC power converter. BESS have been mostly employed in islanded microgrids to store excess renewable generation, see e.g., [4]. However, due to their decreasing cost, they are becoming of increasing interest in grid-connected systems to perform dispatchability, peak shaving, voltage control, and self-consumption of local distributed generation, see e.g [5]–[11].

On the other hand, A ST is a three-stage power electronics transformer that transforms the voltage from the MV to the LV grid [12], [13] and makes available the DC grid connections [14]. It allows to provide new services to distribution grids, like load identification and control [15], and offers new solutions to current problems, like the possibility to deal with reverse power flow conditions [16]. The ST decouples the MV and LV grid. The main constraint that STs must respect is the active power demand from the LV grid, while voltage amplitude and frequency in LV side and reactive power injection in MV side represent degrees of freedom for the grid management.

Research supported by the Swiss Competence Center on Energy Research (SCCER-FURIES).

In this paper, we merge the capabilities provided by the two technologies by proposing a control strategy for the power converters of a ST with integrated BESS. The control objective is twofold: *i)*, achieving dispatched-by-design operation of the active power flow of the LV side and, *ii)*, providing support to voltage regulation to both medium and low voltage side. The control performance is validated in simulations by considering the IEEE 34 nodes test feeder and the CIGRE reference network for LV systems suitably interfaced with a ST.

This paper is organized as follows: Section II describes into details the problem statement and introduces the notation; Section III presents the formulation of the control problems, while Section V shows the simulation results. Finally, Section VI summarizes the main contributions of this work and states the conclusions.

II. Problem Statement and notation

A. Problem statement

We consider the configuration reported in Fig. 1. It consists in a low voltage distribution network interfaced with a medium voltage system through a ST, the setup of which is augmented by including a BESS directly connected to its DC bus. The presence of the ST with storage allows to decouple the two electrical systems both in terms of reactive and active power flows, the latter within the limits imposed by the BESS capacity. The problem tackled in this paper is determining real-time active and reactive power set-points of the MV converter and voltage set-points of the LV converter such that:

1) the active power flow on the MV side is controlled in order to follow the so-called *dispatch plan*, i.e., a sequence of average power consumption profile at 5 minute resolution established the day before operation; the motivation for dispatching the operation of the LV network is that it is a bottom-up approach to decrease the amount of regulating power required to operate the grid.
2) the reactive power injection of the MV converter is controlled to provide voltage regulation support to the MV network;
3) the voltage reference of the LV converter is controlled to provide voltage regulation to the LV network.

At the current stage, we assume that the location of the ST with storage is given. Voltage control requires the knowledge of the voltage levels of both the MV and LV buses, which are assumed known from, for example, PMU-based and smart meters-based monitoring infrastructure or integrated from state estimation algorithms in case of non complete observability, see e.g., [17], [18].

B. Notation and working hypothesis

The MV and LV networks are with M and L buses, respectively. The voltage magnitude of a given node is denoted by $V_{\text{MV},m}$ for the MV network and by $V_{\text{LV},l}$ for the LV. The complex power injections are $P_{\text{MV},m} + jQ_{\text{MV},m}$ and $P_{\text{LV},l} + jQ_{\text{LV},l}$ for MV and LV network, respectively. The quantity V^* denotes the direct sequence voltage of the slack bus for both grids.

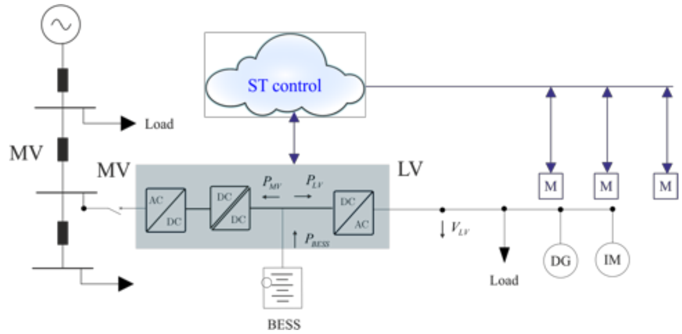

Fig. 1. The considered setup. From the left to the right: a MV network, the smart transformer (ST) with integrated storage and a LV network, whose injections are monitored with smart meters.

III. Methods

Two control problems, one for the MV and the other for the LV network, are formulated.

A. Control Problem on the MV side

The hierarchical control strategy for the MV converter accomplishes the following tasks in a sequential fashion[1]:

1) the active power injection $P_{\text{MV, ST}}$ at the ST bus is determined in order to achieve dispatched-by-design operation of the underneath distribution system. In other words, the active power flow at the ST bus should follow a sequence of average power consumption values at 5 minutes resolution[2], called *dispatch plan* (denoted by the sequence $\widehat{P}_1, \dots, \widehat{P}_{288}$), established the day before the operation. The dispatch plan is defined using the method proposed in [6]. It consists in the additive contribution of two terms: the expected value of the prosumption[3], generated by a forecasting tool, and the offset profile, which accounts for the electricity required to restore a suitable BESS state-of-charge (SOC) and achieve a suitable level of flexibility along the day of operation. In this work, the dispatch plan is assumed given. The decision problem to determine the active power injection is discussed in III-A1;
2) once the active power injection $P_{\text{MV,ST}}$ has been determined, the reactive power injection $Q_{\text{MV,ST}}$ of the power converter is controlled in order to provide primary voltage control to the MV grid. In particular, the optimal reactive power injection is computed by solving a linearized optimization problem while obeying to the

[1]It is hierarchical because the active and reactive power set-points are computed sequentially.

[2]Five minute is chosen because it is a period commonly adopted in real-time elecricity market. This would require an adapation of the existing smart metering infrastructure, which is normally with a reporting rate of 4 frames per hour.

[3]The term "prosumption" denotes the aggregated active power flow of a set of heterogeneous noncontrollable stochastic resources, such as the active power flow of a building equipped with a rooftop PV installation.

power converter operational limits, namely the apparent power should fall in the PQ capability plane of the converter. The objective is to minimize the voltage deviations of the MV network buses from the network rated value, subject to the capability curve of the converter. The detailed formulation of the optimal voltage control problem is described in III-A2.

1) Control of the active power flow on the MV side to achieve dispatched-by-design operation: During real-time operation, the active power flow at the ST bus is given by the sum of the active power flow of the underneath distribution systems and the charge/discharge power required by the BESS, i.e. the quantity we control in order to track the dispatch plan. The control problem consists in a model predictive control strategy actuated with 10 sec resolution which determines the BESS charge/discharge current in order to minimize the mismatch between the 5-minute average active power flow realization and the dispatch plan, while obeying to BESS operational constraints (i.e., BESS current, voltage and state-of-charge should be in their respective range). The control problem formulation, which is omitted here for a reason of space, is according to what proposed and experimentally validated in [6].

2) Control of the reactive power flow on the MV side for voltage support: Once the active power injection $P_{\text{MV,ST}}$ is determined, the reactive power injection $Q_{\text{MV,ST}}$ is computed by solving a constrained optimization problem with the objective of reducing the voltage deviations of the network buses from the network rated value (1 p.u.), as described in the following. Assuming to know from measurements or a state estimation process the state of the network, i.e., the phase-to-ground voltage phasors, the voltage sensitivity coefficients of all the network nodes with respect to absorbed/injected reactive power of the BESS are:

$$K_{Q,m} := \frac{\partial V_{\text{MV},m}}{\partial Q_{\text{MV,ST}}}, \qquad m = 1, \dots, M. \tag{1}$$

and are computed by solving the linear system of equations presented in [19]. Once the sensitivity coefficients are available, we compute the optimal required reactive power adjustments $\{\Delta(Q_{\text{MV,ST}})^*(t)\}$ which lead to the desired operational set-point for voltage control via the following constrained optimization problem:

$$\min_{\Delta Q_{\text{MV,ST}}} \left\{ \sum_{m=1}^{M} \left(V_{MV,m} + K_{Q,m} \Delta Q_{\text{MV,ST}} - V^*\right)^2 \right\} \tag{2}$$

subject to

$$P^2_{\text{MV},ST} + Q^2_{\text{MV,ST}} \leq S_{\text{nom}} \tag{3}$$

where S_{nom} is the nominal apparent power of the MV converter. Its value is normally a dynamic function of the converter operating conditions, like the terminal voltage on the AC side. At this stage, we consider it constant. The inclusion of more representative models will be considered in future work. It is worth noting that the active power $P_{\text{MV,ST}}$ is an input of the problem because it is given by the dispatch operation.

B. Control Problem on the LV side

The ST achieves to provide primary voltage control to the LV grid by setting the voltage reference at the root of the feeder, in a similar way af it were a transformer with on-load tap changing capability. This allows to assure suitable voltage levels along the network buses. In order to do so, we compute the direct sequence voltage sensitivity coefficients of all the network nodes with respect to the reference voltage of the LV grid:

$$K_{V^*,m} := \frac{\partial V_{LV,m}}{\partial V^*}, \qquad m = 1, \dots, L. \tag{4}$$

Sensitivity coefficients in (4) are obtained by solving a linear system of equations (similar to the previous case of voltage sensitivities) with respect to transformer's tap changers positions (e.g., section II.C in [19], or [20] for another example). Once the coefficients are known, the suitable voltage level of the slack bus is determined by the following optimization problem:

$$\min_{\Delta V^*} \left\{ \sum_{m=1}^{M} \left(V_{LV,m} + K_{V^*,m} \Delta V^* - V^*\right)^2 \right\}. \tag{5}$$

The computation of the sensitivity coefficients in (4) requires the knowledge of the LV voltage levels, which are assumed known from smart meters readings or a state estimation process.

IV. Performance Metrics

To measure the performance of the dispatch-by-design strategy, we evaluate the accumulated absolute value of the deviation between the active power flow realization $P(t)$ and dispatch plan $\widehat{P}(t)$ and time t:

$$m_0 = \sum_{t=0}^{T} \left| \widehat{P}(t) - P(t) \right| \tag{6}$$

which is an indicator of the amount of imbalances generated by this portion of the network. The performance of voltage control is measured by comparing the mean $\overline{m}_1$, and maximum $m_1^{\uparrow}$ of the voltage deviations of the buses with respect to the reference value 1 p.u. With reference to the MV network, we denote with $\mathcal{D}$ the set of voltage deviations for all the buses $l = 1, \dots, M$ and time intervals $t = 1, \dots, T$:

$$\mathcal{D} = \left\{ \left(V_{\text{MV},l}(t) - 1\right), t = 1, \dots, T, l = 1, \dots, M \right\}. \tag{7}$$

The formal definitions of the two metrics for the voltage (previously defined in a verbose manner) are:

$$\overline{m}_1 = \frac{1}{T} \frac{1}{L} \sum_{d \in \mathcal{D}} d \tag{8}$$

$$m_1^{\uparrow} = \max \left\{ |d|, \forall d \in \mathcal{D} \right\}. \tag{9}$$

For the LV network, the computation is analogue and obtained by considering in the set $\mathcal{D}$ the voltage levels of the LV buses.

V. Simulation Results

A. Simulation Setup and Procedure

We consider a MV network, where one of the nodes is interfaced with the underneath LV grid through a ST with integrated BESS. The location of the node with the ST is chosen as the node with the largest reactive power sensitivity coefficient, such that its support to the MV network voltage regulation is the most effective.

The MV network is simulated with the IEEE 34 nodes reference network [21]. The injections of the MV nodes are modeled in terms of aggregated active/reactive power flows profiles as defined in the standard, unless for the node equipped with the ST with BESS, which is modelled in details by using the CIGRE LV benchmark grid [22]. The presence of the ST allows to decouple the active and reactive power flows of the two networks, which are therefore simulated separately. The behaviour of the ST with integrated storage is modelled in terms of the power flow injections to the MV and LV networks. The power converter on the MV side is controlled by enforcing active/reactive power references (determined as discussed in III-A), while the LV power converter is controlled to keep a certain voltage level, which is given as described in III-B. The control logic of power converters is not simulated. At this stage, the efficiency of the power conversion is assumed unitary. Both MV and LV networks are simulated with three-phase power flows. The rated power of the ST power converters is 720 kVA and the storage capacity is assumed 500 kWh.

The relevant inputs for the networks simulations are according an educated guess. They are:

- For the MV grid: reference profiles are according to experimental measurements from a test network of compatible size, unless for the MV/LV interface, where it is as the dispatch plan. Loads are unbalanced.
- For the LV grid: the active power flow injections at the buses are obtained starting from the time varying profile proposed by CIGRE network specifications scaled down according to the nominal power of each node. Reactive flows are calculated assuming a constant power factor (0.9). However, the magnitude of the injections are deliberately enlarged with the objective of inducing violations of the voltage constraints when the control strategy is not actuated. This is with the specific objective of showing the capability of the proposed control to improve voltage levels. The dispatch plan at the MV/LV interface (which is normally generated by integrating forecast of the prosumption, as explained in the foregoing) is given by the sum of the single injections at the buses plus a random component to simulate forecast uncertainties. Loads are assumed balanced.

B. Case studies

Two cases are considered:

1) **Case 0** (base case). The ST with storage at the selected MV bus is not available. Therefore, the operation of the selected MV node is not dispatched by design (i.e., its flow is stochastic rather than being according to a pre-established profile), and voltage support is not provided to either the MV or LV network.
2) **Case 1**. The ST with storage at the selected MV bus is available and controlled as discussed in Section III to provide dispatched-by-design operation of the selected MV node and voltage support to both the MV and LV networks.

C. Simulations Results

Simulation results are shown in Figures from 2 to 5. Fig. 2 shows the active power flow on the MV side of the smart transformer for Case 0 and Case 1 compared to the dispatch plan. It is visible that in Case 1, the control strategy achieves the power flow to track the dispatch plan, compared to when the control is not active, where the flow is stochastic because it follows its natural pattern. The values of metric m_0 (in kWh) calculated for both cases are summarized in Table I: they denote that the cumulative sum of the absolute value of the tracking error is nearly zero for Case 1, while it is considerably larger for Case 0.

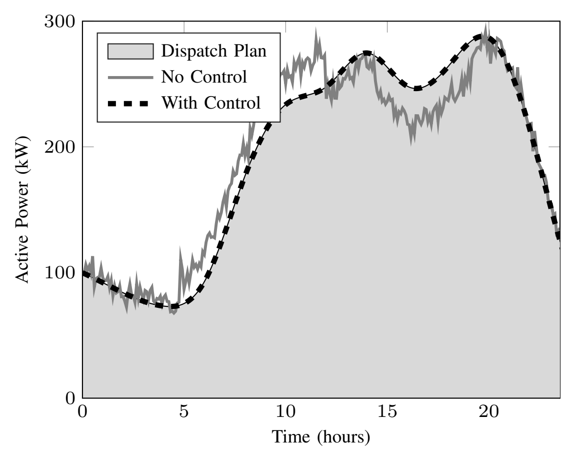

Fig. 2. Active power flow on the MV side of the ST in the case without (full line, Case 0) and with control (dashed, Case 1): in the latter case, it corresponds to the *dispatch plan*, which is computed the day before the operation.

TABLE I
Dispatch performance

Metric	**Case 0**	**Case 1**
m_0 (kWh)	370.74	0.089

Fig. 3 shows the reactive power flow at the MV bus of the ST before and after the proposed control action is actuated. The effects on the MV voltage levels are discussed in the following paragraph.

Figures 4 and 5 are the boxplots (mean, standard deviation and outliers) of the voltage values on the MV buses for Case 0 and Case 1, respectively. Table II summarizes the voltage control performance metrics. Voltage levels are substantially

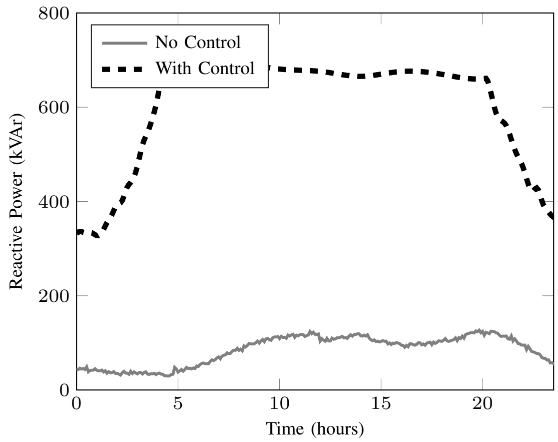

Fig. 3. Reactive power flow on the MV side of the ST before (full line, Case 0) and after the control action (dashed, Case 1).

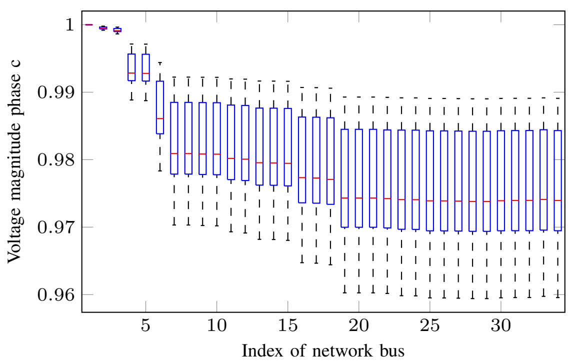

Fig. 4. MV network, Case 0: boxplot of the voltage levels along the buses (phase C) of the MV network in the uncontrolled case.

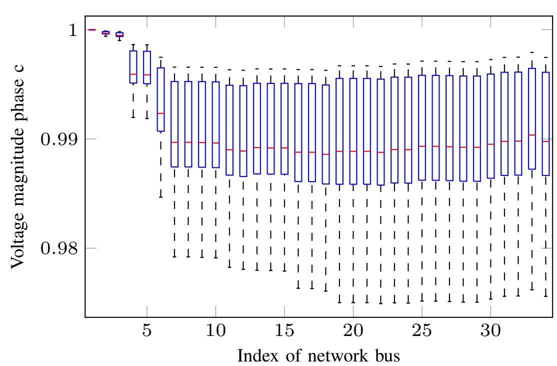

Fig. 5. MV network, Case 1: boxplot of the voltage levels along the buses (phase C) of the MV network in the controlled case.

TABLE II
MV NETWORK: VOLTAGE CONTROL PERFORMANCE

Metric	**Case 0**	**Case 1**
$\overline{m}_1$	-1.08%	-0.11%
$m_1^{\uparrow}$	4.06%	2.51%

improved thanks to the actuation of the proposed control action.

Fig. 6 compares the voltage profile on the LV slack bus before and after the actuation of the proposed control action that, recalling from the Methods section, is computed with the objective of improving the voltage levels in the LV on a best effort basis. The effects on the voltage levels in the LV network are discussed hereafter.

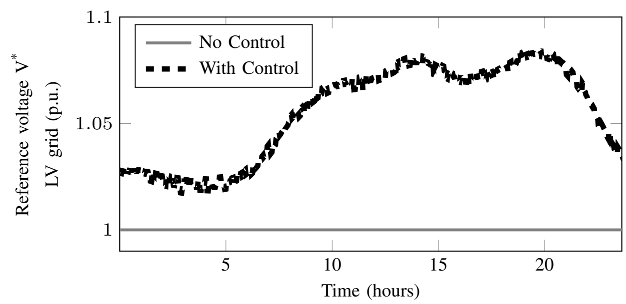

Fig. 6. Evolution in time of the voltage level imposed by the ST on the LV slack bus before and after the control action.

The voltage levels on the LV buses before and after the actuation of the proposed control action are shown in figures 7 and 8, respectively. As visible in Fig. 7, voltage levels in the uncontrolled case are far from being acceptable, whereas they appear substantially improved in Fig. 8 after the actuation of the control action. Metrics of voltage control performance are summarized in Table III and confirm a marked improvement of the voltage values, thus denoting the capability of the proposed control strategy to control the voltage.

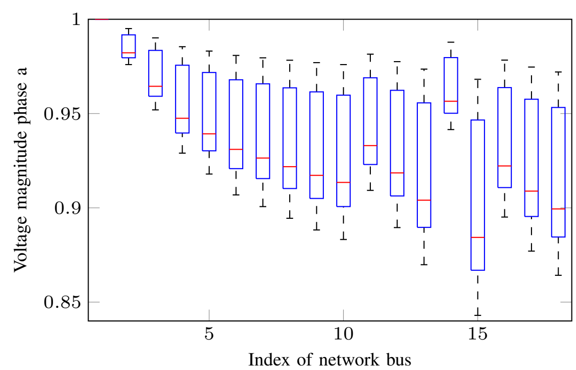

Fig. 7. LV network, Case 0: boxplot of the voltage levels along the buses (phase A) of the LV network in the uncontrolled case.

TABLE III
LV NETWORK: VOLTAGE CONTROL PERFORMANCE

Metric	**Case 0**	**Case 1**
$\overline{m}_1$	-5.92%	0.03%
$m_1^{\uparrow}$	15.96%	8.45%

VI. CONCLUSIONS AND FUTURE WORKS

A control strategy for a LV/MV smart transformer with integrated storage was proposed. On the MV side, it controls

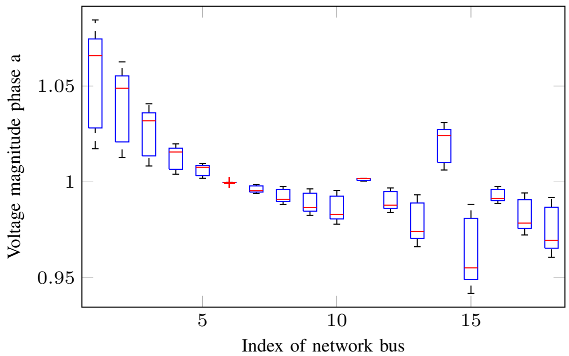

Fig. 8. LV network, Case 1: boxplot of the voltage levels along the buses (phase A) of the LV network in the controlled case.

i) the active power flow of the power converter to achieve dispatched-by-design operation of the LV feeder (namely, its active power flow follows a sequence of average power consumption value at 5 minutes resolution established the day before operation), and ii) the reactive power injection in order to provide voltage regulation to the MV network on a best effort basis. On the LV side, it controls the voltage at the root of the feeder to assure suitable voltage levels along the line.

Thanks to the capability of the selected configuration to fully decouple the active and reactive power flows of the LV and MV grids (in the limits imposed by the battery capacity and power converters capability curves), the aforementioned control objectives are independent. This is an advantage compared to, for example, multi-objective optimizations with conventional setups, where a trade-off between the control performance is normally to expect.

The control performance is validated in simulations by considering the IEEE 34 nodes test feeder and the CIGRE reference network for LV systems. Simulation results show the capability of the proposed strategy to improve voltage levels of both the MV and LV network and achieve dispatched-by-design operation of distribution systems.

The future work is in the direction of a more detailed modelling of the power converters with the objective of integrating it in the model predictive control framework.

REFERENCES

[1] N. Jenkins, R. Allan, P. Crossley, K. D., and S. G., *Embedded Generation*. The Institution of Electrical Engineers, London, 2000.

[2] J. P. Lopes, N. Hatziargyriou, J. Mutale, P. Djapic, and N. Jenkins, “Integrating distributed generation into electric power systems: A review of drivers, challenges and opportunities,” *Electric Power Systems Research*, vol. 77, no. 9, pp. 1189 – 1203, 2007, distributed Generation. [Online]. Available: http://www.sciencedirect.com/science/article/pii/S0378779606001908

[3] S. Sarri, M. Paolone, R. Cherkaoui, A. Borghetti, F. Napolitano, and C. A. Nucci, “State estimation of active distribution networks: Comparison between wls and iterated kalman-filter algorithm integrating pmus,” in *2012 3rd IEEE PES Innovative Smart Grid Technologies Europe (ISGT Europe)*, Oct 2012, pp. 1–8.

[4] R. Palma-Behnke, C. Benavides, F. Lanas, B. Severino, L. Reyes, J. Llanos, and D. Sáez, “A microgrid energy management system based on the rolling horizon strategy,” *IEEE Transactions on Smart Grid*, vol. 4, no. 2, pp. 996–1006, June 2013.

[5] C. A. Hill, M. C. Such, D. Chen, J. Gonzalez, and W. M. Grady, “Battery energy storage for enabling integration of distributed solar power generation,” *IEEE Transactions on Smart Grid*, vol. 3, no. 2, pp. 850–857, June 2012.

[6] F. Sossan, E. Namor, R. Cherkaoui, and M. Paolone, “Achieving the dispatchability of distribution feeders through prosumers data driven forecasting and model predictive control of electrochemical storage,” *IEEE Transactions on Sustainable Energy*, vol. 7, no. 4, pp. 1762–1777, Oct 2016.

[7] M. A. Abdullah, K. M. Muttaqi, D. Sutanto, and A. P. Agalgaonkar, “An effective power dispatch control strategy to improve generation schedulability and supply reliability of a wind farm using a battery energy storage system,” *IEEE Transactions on Sustainable Energy*, vol. 6, no. 3, pp. 1093–1102, July 2015.

[8] E. Namor, D. Torregrossa, F. Sossan, R. Cherkaoui, and M. Paolone, “Assessment of battery ageing and implementation of an ageing aware control strategy for a load leveling application of a lithium titanate battery energy storage system,” in *2016 IEEE 17th Workshop on Control and Modeling for Power Electronics (COMPEL)*, June 2016, pp. 1–6.

[9] K. Christakou, D.-C. Tomozei, M. Bahramipanah, J.-Y. Le Boudec, and M. Paolone, “Primary voltage control in active distribution networks via broadcast signals: The case of distributed storage,” *IEEE Transactions on Smart Grid*, vol. 5, no. 5, pp. 2314–2325, 2014.

[10] C. T. Li, H. Peng, and J. Sun, “Mpc for reducing energy storage requirement of wind power systems,” in *2013 American Control Conference*, June 2013, pp. 6607–6612.

[11] M. Marinelli, F. Sossan, G. T. Costanzo, and H. W. Bindner, “Testing of a predictive control strategy for balancing renewable sources in a microgrid,” *IEEE Transactions on Sustainable Energy*, 2014.

[12] M. Liserre, G. Buticchi, M. Andresen, G. De Carne, L. Costa, and Z.-X. Zou, “The smart transformer, its impact on the electric grid and its technology challenges,” *IEEE Trans. Ind. Electr. Mag.*, in press 2016.

[13] X. She, A. Huang, and R. Burgos, “Review of solid-state transformer technologies and their application in power distribution systems,” *IEEE Journal of Emerging and Selected Topics in Power Electronics*, vol. 1, no. 3, pp. 186–198, Sept 2013.

[14] G. Buticchi, G. D. Carne1, D. Barater, Z. Zou, and M. Liserre, “Analysis of the frequency-based control of a master/slave micro-grid,” *IET Renewable Power Generation*, in press.

[15] G. D. Carne, G. Buticchi, M. Liserre, and C. Vournas, “Load control using sensitivity identification by means of smart transformer,” *IEEE Transactions on Smart Grid*, vol. PP, no. 99, pp. 1–1, 2016.

[16] L. M. Cipcigan and P. C. Taylor, “Investigation of the reverse power flow requirements of high penetrations of small-scale embedded generation,” *IET Renewable Power Generation*, vol. 1, no. 3, pp. 160–166, September 2007.

[17] P. A. Pegoraro, J. Tang, J. Liu, F. Ponci, A. Monti, and C. Muscas, “Pmu and smart metering deployment for state estimation in active distribution grids,” in *Energy Conference and Exhibition (ENERGYCON), 2012 IEEE International*. IEEE, 2012, pp. 873–878.

[18] S. Sarri, M. Paolone, R. Cherkaoui, A. Borghetti, F. Napolitano, and C. A. Nucci, “State estimation of active distribution networks: Comparison between wls and iterated kalman-filter algorithm integrating pmus,” in *2012 3rd IEEE PES Innovative Smart Grid Technologies Europe (ISGT Europe)*. IEEE, 2012, pp. 1–8.

[19] K. Christakou, J. Y. LeBoudec, M. Paolone, and D. C. Tomozei, “Efficient computation of sensitivity coefficients of node voltages and line currents in unbalanced radial electrical distribution networks,” *IEEE Transactions on Smart Grid*, vol. 4, no. 2, pp. 741–750, June 2013.

[20] G. D. Carne, M. Liserre, and C. Vournas, “On-line load sensitivity identification in lv distribution grids,” *IEEE Transactions on Power Systems*, vol. PP, no. 99, pp. 1–1, 2016.

[21] W. H. Kersting, “Radial distribution test feeders,” in *Power Engineering Society Winter Meeting, 2001. IEEE*, vol. 2. IEEE, 2001, pp. 908–912.

[22] S. Papathanassiou, N. Hatziargyriou, K. Strunz *et al.*, “A benchmark low voltage microgrid network,” in *Proceedings of the CIGRE symposium: power systems with dispersed generation*, 2005, pp. 1–8.